Mechanical characterization of polymers with enhanced thermal conductivity

1. Introduction

Polymer properties can easily be adjusted by compounding, a process in which fillers are mixed into the polymer matrix to adapt the desired property. This is often done to increase the low thermal conductivity of polymers which is typically in the range of 0.1 W/(mK) to 0.5 W/(mK) [1]. Metal (e.g. aluminum, copper, zinc), carbon (e.g. graphite, graphene, carbon black) and mineral fillers (e.g. boron nitride, aluminum nitride, talc) are usually applied to enhance the polymer's thermal conductivity. However, when particles are mixed into a polymeric matrix, the interaction between the particles and the polymer does not only affect the thermal conductivity but also the mechanical properties. In general, the incorporation of a filler into a polymeric matrix decreases the ultimate tensile strength and the strain at break [2]. This is due to the formation of stress concentration sites [3]. Furthermore, the Young's modulus is increased as the compound stiffens by the incorporation of fillers. However, there is no generally applicable theory for the stress-strain behavior of a filled system. Thus, the present study investigated the mechanical properties of polymers with enhanced thermal conductivity.

The first part of the research focused on the influence on the mechanical properties when different types of fillers with a high thermal conductivity are added to high-density polyethylene (HDPE). The fillers (aluminum, boron nitride, copper, expanded graphite, natural graphite) were chosen due to their high efficiency in enhancing the initially low thermal conductivity of HDPE which is approximately 0.5 W/(mK) [1]. Tensile testing was applied to find the Young's modulus, the strain at break and the ultimate tensile strength. Via Charpy impact testing, the impact strength of notched and unnotched specimens and the notch sensitivity of the compounds were found.

The type of dispersion, the particle agglomeration, the size and the shape of fillers are important factors that determine the mechanical properties of two-phase systems [4][5]. The expanded graphite particles changed their shape and size during compounding as they proved to be sensitive towards the applied shear. Thus, the second part of the present study focused on investigating the influence of processing on the mechanical characteristics of compounds containing expanded graphite. In general, two types of compounding are available. Whereas direct compounding simply blends the filler and the polymer in a single extrusion round, the compounding via masterbatch involves two extrusion rounds. In the first extrusion round, a compound with a high filler content is produced which is further diluted to the desired filler content in a second extrusion round. Thus, the material undergoes a high load of shear twice. For materials which are sensitive towards shear this might also affect the mechanical properties. Again, tensile testing and Charpy impact testing were applied to investigate a possible impact on those properties.

2. Experimental

2.1. Materials

The commercially available high-density polyethylene (HDPE) grade Bormed™ HE9621-PH with a melt flow rate of 12 g/min (2.16 kg, 190 °C) and a density of 0.964 kg/m³ was generously provided by Borealis GmbH (Linz, AT) and used as received. The HDPE was used as base material for all compounds. Via compounding, different fillers were mixed into the HDPE matrix. The filler contents for the materials screening and the investigation of the processing impact are given in the following.

2.1.1. Materials screening

The first part of the study will be referred to as the "material screening" as different types of fillers are investigated. For this purpose, compounds with filler contents of 10 vol%, 20 vol% and 30 vol% of aluminum, boron nitride, copper, expanded graphite and natural graphite were prepared. Including the unfilled polymer, this gives a total of 16 materials. All fillers were used as received without any surface treatment. The fillers along with their abbreviation, their average particle size, their specific surface and their density and their shape are given in Table 1. Each compound will be referred to as the filler abbreviation and the filler content in vol%. For example, the HDPE-based compound containing 10 vol% of aluminum will be called A10.

Table 1: Fillers and their used abbreviation along with their average particle size, their specific surface and their density and their shape

Filler (abbreviation)	Average particle size [µm]	Specific surface [m²/g]	Density [kg/m³]	Shape
Aluminum (A)	35-45	1.29	2.7	Flakes
Boron nitride (BN)	50	-	2.25	Flakes
Copper (C)	> 45	430	8.9	Flakes
Expanded graphite (EG)	1200	18-20	2.2	Flakes
Natural graphite (G)	5-6	4500-5100	2.2	Flakes

2.1.2. Processing impact

The second part of the study will be referred to as the "processing impact". For this purpose, compounds with filler contents of 3 vol% and 5 vol% for each expanded graphite type (small, medium-sized and large particles) were compounded via two different processing ways as described in more detail in 2.2.2. This gives a total of 12 materials. All fillers were used as received without any further surface treatment. The types of expanded graphite along with their average particle size, their density and their shape are given in Table 2. Each compound will be referred to as the type of expanded graphite (EG-S = small, EG-M = medium-sized and EG-L = large particles), the filler content in vol% and the type of processing ("dir" for direct processing and "MB" for processing via masterbatch). For example, the HDPE-based compound containing 5 vol% of the small expanded graphite particles and processed via masterbatch will be called EG-S-5-MB.

Table 2: The expanded graphite types along with their average particle size, their density and their shape

Expanded graphite type	Average particle	Density [kg/m³]	Shape

	size [µm]		
EG_S	130	2.2	Flakes
EG-M	600	2.2	Flakes
EG-L	1200	2.2	Flakes

2.2. Compound fabrication and specimen preparation

The compounding was done on a co-rotating twin screw compounder (Werner & Pfleiderer GmbH, Dinkelbühl, DE) with an L/D ratio of 38 and equipped with 6 control zones, a gravimetric dosing unit, side feeding, vacuum degassing, a cool bath and strand pelletizing. The temperature of the six control zones were set to 140 °C, 180 °C, 190 °C, 190 °C, 190 °C and 190 °C and the screw speed was set to 200 rpm for all compounds. Depending on the filler type and filler content, different parameters were chosen for the mass feed rates of the main dosing unit from which the polymer was added and for the mass feed rates of the side dosing unit from which the fillers where added into the compounder. Those and the according wt-% as converted from the vol% are given in the following.

2.2.1. Material screening

The main dosing unit was used for adding the polymer and the side dosing unit was used for adding the filler. The filler contents in vol% and the according filler contents in wt%, the mass feed rates of the main dosing unit, the side dosing unit and of the compounder are given in Table 3.

Table 3: Processing parameters of the compounds from the material screening: filler, filler content in vol%, filler content in wt.-%, mass feed rate of the main dosing unit, mass feed rate of the side dosing unit and the total mass feed rate of the compounder

Filler	Filler content [vol%]	Filler content [wt.-%]	Mass feed rate main dosing unit [kg/h]	Mass feed rate side dosing unit [kg/h]	Mass feed rate compounder [kg/h]
Aluminum	10	24	4.56	1.44	6
	20	41	2.95	2.05	5
	30	55	2.25	2.75	5
Boron nitride	10	21	4.74	1.26	6
	20	37	2.52	1.48	4
	30	50	2	2	4
Copper	10	51	2.94	3.06	6
	20	70	2.7	6.3	9
	30	80	2	8	10
Expanded graphite	10	20	4.56	1.44	5
	20	36	3.2	1.8	5
	30	50	3	3	6
Natural graphite	10	20	7.2	1.8	9
	20	36	3.7	1.8	5
	30	50	2	2	4

2.2.2. Processing impact

To investigate a possible impact of the processing, compounds containing the same amount of expanded graphite were processed in two different ways, the first one being direct compounding via the main dosing unit for the polymer and side dosing unit for the filler as seen for the materials screening in 2.2.1. Processing parameters such as the filler contents in vol% and in wt%, the mass

feed rates of the main dosing unit, the side dosing unit and of the compounder for the direct processing are given in Table 4.

Table 4: Processing parameters for compounds containing different types of expanded graphite which were processed directly: the type of expanded graphite, the filler content in vol%, the filler content in wt%, the mass feed rate of the main dosing unit, the mass feed rate of the side dosing unit and the total mass feed rate of the compounder

Expanded graphite type	Filler content [vol%]	Filler content [wt.-%]	Mass feed rate main dosing unit [kg/h]	Mass feed rate side dosing unit [kg/h]	Mass feed rate compounder [kg/h]
EG-S	3	6.6	8.406	0.594	9
EG-S	5	10.8	6.244	0.756	7
EG-M	3	6.6	6.538	0.462	7
EG-M	5	10.8	6.244	0.756	7
EG-L	3	6.6	6.538	0.462	7
EG-L	5	10.8	4.46	0.54	5

For the second type of processing, a masterbatch (MB) containing 8.7 vol% (18 wt%) of the according expanded graphite type was compounded in a first step (mass feed rate dosing unit = 6.56 kg/h; mass feed rate side feeding = 1.44 kg/h). The granules of the MB and the granules of the HDPE were then dry blended and compounded again. The expanded graphite type, the filler content in vol%, the according filler content in wt%, the proportion of the masterbatch for dry blending, the proportion of the HDPE for dry blending and the total mass feed rate of the compounder are given in Table 5.

Table 5: Processing parameters for compounds containing different types of expanded graphite which were processed via a masterbatch: the type of expanded graphite, the filler content in vol%, the filler content in wt%, the proportion of the masterbatch for dry blending, the proportion of the HDPE for dry blending and the total mass feed rate of the compounder

Expanded graphite type	Filler content [vol%]	Filler content [wt.-%]	Masterbatch for dry blending [wt.-%]	HDPE for dry blending [wt.-%]	Mass feed rate main dosing unit = total mass feed rate compounder [kg/h]
EG-S	3	6.6	63.33	36.67	8
EG-S	5	10.8	40	60	8
EG-M	3	6.6	63.33	36.67	10
EG-M	5	10.8	40	60	10
EG-L	3	6.6	63.33	36.67	12
EG-L	5	10.8	40	60	10

The unfilled HDPE and the compound granules were then compression molded under vacuum atmosphere into 160 mm * 160 mm plates with a height of 4 mm. Therefore a vacuum press P 200 PV (Dr. Collin GmbH, DE) was applied. The applied compression molding parameters are summarized in Table 6.

Table 6: The temperature, the time and the machine pressure for the 5 different segment during the compression molding of the sample plates

Pressing segment	1	2	3	4	5
Temperature [°C]	200	200	200	200	30

Time [min]	20	5	3	1	10
Machine pressure [bar]	1	100	150	200	200

After compression molding, the plates were cut with an abrasive water jet cutter Maxiem 0707 (Omax Corporation, Kent, US) to the adequate specimen dimensions for the tensile testing and for the Charpy impact testing according to ISO 527 (specimen 1B, “dogbone”) and ISO 179 (specimen U and A), respectively. The edges of the specimens were deburred with a fine abrasive paper if necessary. The notch for specimen A of the Charpy impact testing was made with a notching machine Notchvis (CEAST/Instron, Norwood, US).

2.3. Tensile testing

Tensile testing was done on a universal testing machine 4202 (Instron, Norwood, US). A load cell with a maximum load of ca. 9000 N (=2000 lbs) and general purpose static tension grips were used. A standalone digital controller eP2 (ADMET, Norwood, US) was connected to the load frame and a computer and served as interface in between those. The software GaugeSafe (ADMET, Norwood, US) was used for setting the testing parameters and for collecting the data of the force signal and the crosshead displacement. An experimental setup with a high-resolution, monochrome scientific camera Chameleon3 (FLIR Systems, Inc., Wilsonville, US) was used for detecting the strain. Therefore, two lines at the upper and lower limit of the parallel sided part of the specimen (length = 60 mm) were marked with a color that was easily distinguishable from the texture of the specimen. The camera was placed in front of the load frame and adequate illumination was installed as displayed in Figure 1. High-resolution images were taken with a framerate of 5 frames per second during each measurement. A selfwritten program linked the recorded images to the force signal. In order to get the according strain, the software evaluated the movement of the marked lines via an edge-finding algorithm. Edges were detected when a high contrast (e.g. silver marker on black specimen as displayed Figure **1**) was present. The strain could then be correlated with the force signal from the load frame in order to obtain the strain-stress plot of the tensile test. At least 10 specimens of each material were tested. The presented data represents the average of those measurements and the standard deviations are given along. The specimen dimensions were measured three times at the parallel sided part of the specimen with a caliper and an average value was taken for calculating the stress. A test speed of 1 mm/min was applied for all measurements. The Young’s modulus E, the strain at and ultimate tensile strength were evaluated according to ISO 527.

Figure 1: Experimental setup for the tensile testing. A high-resolution, monochrome camera was placed in front of the load frame to record images during each measurement. The strain was evaluated from the recorded images and it was further correlated with the force signal in order to obtain the stress-strain curve.

2.4. Impact testing

The Charpy impact testing was done on an impact tester Resil 25 (CEAST/Instron, Norwood, US). The specimens were tested flatwise. For each material, 10 unnotched specimens and 9 notched specimens were tested. The presented data represents the average of those measurements and standard deviations are given along. The specimen dimensions were measured with a caliper in the center part of each specimen. The impact pendulums with impact energies of 2 J (unnotched HDPE) and of 0.5 J (all other specimens) were used. The impact strength of the unnotched specimens a_{cU} and the impact strength of the notched specimens a_{cN} were evaluated according to ISO 179. Furthermore, the notch sensitivity k_Z was calculated according to equation (1)

$$k_Z = \frac{a_{cN}}{a_{cU}} * 100\% \quad (1)$$

3. Results

3.1. Materials screening

3.1.1. Tensile testing

For the HDPE-based compounds containing different types of fillers of up to 30 vol%, the obtained experimental values of the Young's modulus, the strain at break and the ultimate tensile strength at different filler contents are displayed in the following. Along with the experimental values which are connected by lines to guide the eye but not to represent a function, predictive laws to estimate the mechanical properties of the compounds were applied.

In general, the Young's modulus of a polymeric material increases by the incorporation of particles as its stiffness increases. There are several predictive laws available to estimate the evolution of the Young's modulus in a two-phase system. Einstein's model [6] can only be applied to two-phase systems with a low content of non-interactive particles [7]. It assumes perfect adhesion between the filler and the polymer matrix and a perfect dispersion of the individual particles meaning no interaction between the individual particles. The model predicts the Young's modulus of a compound E_c as given in equation (2),

$$E_c = E_p(1 + 2.5\,\Phi) \tag{2}$$

with E_p as the Young's modulus of the polymer and with Φ as the filler content in vol%. If the matrix slips by the particles instead of adhering to them, a modified version of it can be applied as given in equation (3),

$$E_c = E_p(1 + \Phi) \tag{3}$$

with E_p as the Young's modulus of the polymer and with Φ as the filler content in vol%. The modified equation considers a weak adhesion between the particles and the matrix and a resulting possible break during load is applied. Consequently, the polymer deforms more than the particles and elliptical voids occur around each particle which decreases the Young's modulus with increasing particle content.

The Guth equation is based on the Einstein equation but considers the interaction between particles at higher filler contents [7] and is given in equation (4),

$$E_C = E_P(1 + 2.5\,\Phi + 14.1\,\Phi^2) \tag{4}$$

with E_p as the Young's modulus of the polymer and with Φ as the filler content in vol%.

The Thomas equation is an empirical law which is based on the data generated from a two-phase system with non-agglomerated spherical particles and is given in equation (5),

$$E_C = E_P(1 + 2.5\,\Phi + 10.05\,\Phi^2 - 0.00273\,e^{16.6\,\Phi}) \tag{5}$$

with E_p as the Young's modulus of the polymer and with Φ as the filler content in vol%.

Nielsen's model [8] was applied to estimate the strain at break. It predicts the strain at break of a compound ε_c as given in equation (6)

$$\varepsilon_c = \varepsilon_p(1 - \Phi^{1/3}) \tag{6}$$

with ε_p as the strain at break of the polymer and Φ as the filler content in vol%. However, as Nielsen's model tends to underestimate the decrease in the strain at break as it assumes perfect adhesion between the fillers and the matrix[9], the model developed by Mitsuishi et al. [10] was equally applied. It estimates the strain at break of a compound ε_c as given in equation (7),

$$\varepsilon_c = \varepsilon_p(1 - A\,*\,\Phi^{2/3}) \tag{7}$$

with ε_p as the strain at break of the polymer, Φ as the filler content in vol% and A as constant depending on the filler size and the modification of the filler.

First power laws, two-thirds power laws and their modifications are typically used for predicting the ultimate tensile strength in two-phase systems. They are based on the relation between the area fraction and volume fraction of the inclusions[11]. The first power law represents a completely random distribution of the fillers, whereas the two-thirds power law represents the distribution of spherical inclusions. Typically, weighting factors are added to describe the adhesion. Two different models were applied to estimate the evolution of the ultimate tensile strength for the present study.

Bigg's model[12] considers a possible impact of dewetting due to poor interfacial adhesion or to breaking up of aggregates of fillers with low strength[5]. If no adhesion between the particles is present, Bigg estimates the ultimate tensile strength of a compound σ_c as given in equation (8),

$$\sigma_c = \sigma_p(1 - B * \Phi^{2/3}) \quad (8)$$

with σ_p as the ultimate tensile strength of the polymer, with B as a constant that describes the adhesion quality between the particle and the matrix and with Φ as the filler content in vol%. If there is a dense hexagonal packing in the plane highest density, A equals 1.1. If there is poor adhesion, A equals 1.21. Generally speaking, the lower A below 1.21, the better is the adhesion between the particles and the matrix [9].

The porosity model considers the particles as pores or voids. As it assumes the absence of an adhesion between the particles and the polymer, the pores do not impact the mechanical properties of the compounds. The model predicts ultimate tensile strength of a compound σ_c as given in equation (9),

$$\sigma_c = \sigma_p(e^{-C*\Phi}) \quad (9)$$

with σ_p as the ultimate tensile strength of the polymer, with C as a constant that describes the stress concentration as a result from the pores and with Φ as the filler content in vol%.

3.1.1.1. Young's modulus

In Figure 2 the Young's modulus of the HDPE-based compounds containing different types of fillers along with the estimation according to equations (2), (4) and (5) are given. Due to the difficult and irregular texture of the specimens of certain materials (AP30, C10, C30, G30, EG20, EG30), the strain and therefore the Young's modulus could not be obtained from the recorded images and these values are missing in Figure 2. Therefore, the results of the compounds containing lower filler contents of the expanded graphite (3 vol% and 5 vol% - compounded directly) are additionally given to more easily estimate the evolution of the Young's modulus.

The tensile testing generated a Young's modulus of 1640 MPa for the unfilled HDPE. According to the material data sheet, the Young's modulus of the unfilled HDPE is 1150 MPa. However, this value was determined on injection-molded specimens which typically exhibit different morphology (orientations of the molecular chains in direction of injection and differences in the crystalline morphology). Thus, injection-molded specimens may possess different mechanical properties as compression-molded specimens. Given this fact, the Young's modulus of HDPE determined for the present study and the one from the material data sheet are in reasonable agreement.

For all compounds, the Young's modulus increased with increasing filler content. It was increased in the order from smallest to highest by the incorporation of the following particles: boron nitride, natural graphite, copper, expanded graphite and aluminum. It increased from to 1640 MPa to 2031 MPa, 2979 MPa and 3459 MPa for the BN10, BN20, BN30, to 2170 MPa and 3297 MPa for the G10 and G20, to 3609 MPa for the C20, to 1917 MPa, 2364 MPa and 2730 MPa for the EG3, EG5 and EG10, to 2883 MPa and to 3709 MPa for the A10 and A20, respectively.

Einstein's model which assumes perfect adhesion between the filler and matrix (equation (2)) estimated the increase in the Young's modulus well for the BN10 and G10. However, it underestimated by far the increase in the Young's modulus for all other compounds. Therefore, the modified version of Einstein's model which considers a worse adhesion between the filler and the matrix (equation (3)) is not displayed in Figure 2 as it would underestimate the evolution of the Young's modulus even more. The agreement between the calculated and the measured values for BN10 and G10 at small filler contents is in good agreement that no interaction between the particles is considered for Einstein's model. At higher filler contents, the particles start to interact as more of them are present. Thus, Einstein's model is not applicable anymore. The Guth equation predicts the evolution of the Young's modulus of graphite-filled compounds well but not for the other compounds. The Thomas equation estimates the evolution of the Young's modulus rather well for the boron-nitride filled compounds.

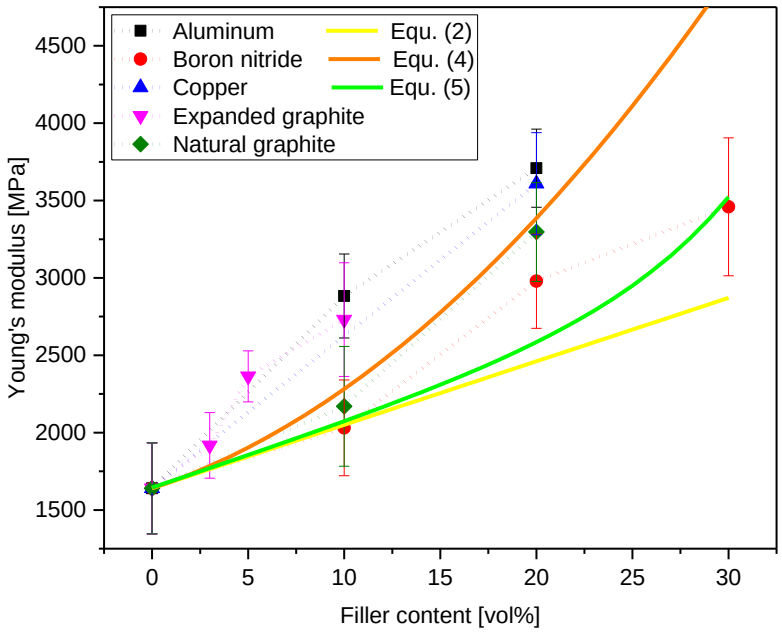

Figure 2: Young's modulus of HDPE-based compounds containing different types of fillers at filler contents up to 30 vol%

3.1.1.2. Strain at break

In Figure 3 the strain at break of the HDPE-based compounds containing different types of fillers along with the estimation according to equations (6) and (7) are given. Due to the difficult and irregular texture of the specimens of certain materials (AP30, C10, C30, G30, EG20, EG30), the strain could not be obtained from the recorded images and these values are missing in Figure 3. Therefore, the results of the compounds containing lower filler contents of the expanded graphite (3 vol% and 5 vol%, compounded directly) are additionally given to more easily estimate the evolution of the strain at break.

An initial strain at break for the unfilled HDPE of 11.2 % was obtained. A high standard deviation was detected as displayed in Figure 4. The depicted curves reflect the lowest (red curve: 7.2 %), the highest (black curve: 16.3 %) and the average (blue curve 11.1 %) strain at break which were detected. Interestingly no yielding occurred during the tensile testing. Yielding is typically expected for HDPE as it is a ductile material. However, the applied HDPE exhibited a degree of crystallinity of about 80 % which is at the upper limit in the typical range the degree of crystallinity of HDPEs (60 % - 80 %)[13]. The higher the degree of crystallinity, the more brittle is the polymer. Furthermore, when

looking at the fracture surface of the specimens (image taken with a light microscope SZX12 (Olympus, Tokyo, JP)), one can clearly see that the crack started at the specimen edge. The rougher surface produced by the water jet cutting seemed to act as crack initiator. Thus, the combination of the high degree of crystallinity and the rough surface on the small side of the specimen inhibited the occurrence of yielding during the tensile test.

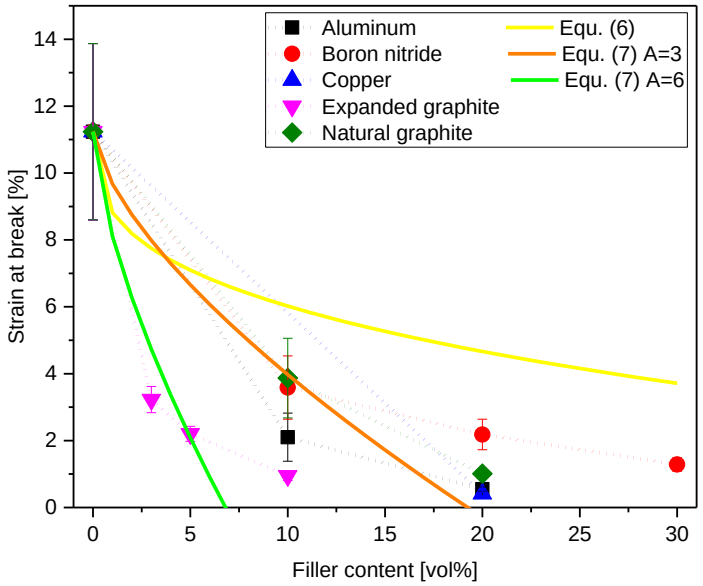

Figure 3: Strain at break of HDPE-based compounds containing different fillers at filler contents up to 30 vol%. It decreased with the incorporation of fillers for all compounds.

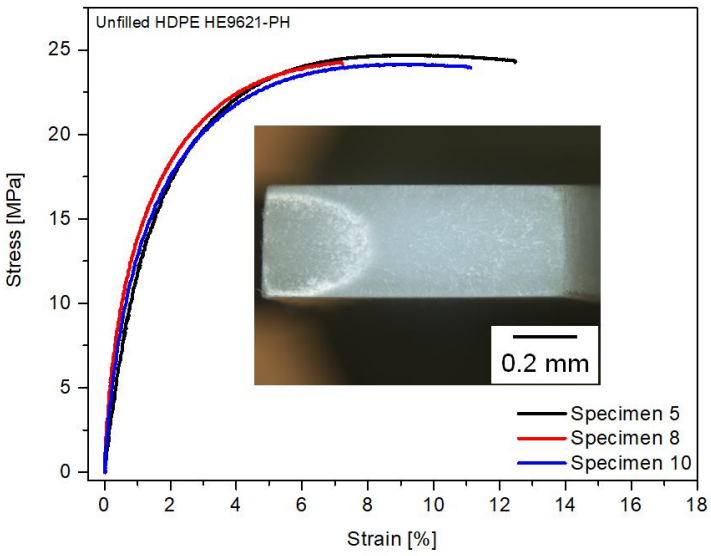

Figure 4: Three representative stress-strain plots of the HE9621-PH and an image of the fracture surface of specimen 5. No yielding of the material was detected. The crack started at the edge of the specimen due to the rougher surface of the cut area when compared to compression-molded area.

For all compounds the strain at break decreased with increasing filler content. It decreased to 2.1 %, 0.5 % for the A10, A20, to 3.6 %, 2.2 %, 1.3 % for the BN10, BN20, BN30, to 0.4 % for the C20, to 3.2 %, 3.3 %, 0.9 % for the EG3, EG5, EG10, and to 3.9 %, 1 %, for the G10, G20. For most of the

compounds, the major decrease in the strain at break was detected by the incorporation of 10 vol% of filler. Whereas the strain at break was decreased by approximately 70 % for the BN10 and G10, it decreased by approximately 80 % and 90 % for A10 and EG10, respectively. Thus, a large embrittlement due to the incorporation of filler took place. However, at the higher filler contents of 20 vol% and 30 vol%, a smaller decrease was detected for all compounds indicating that the main embrittlement occurred until 10 vol%.

The Nielsen model (yellow curve, equation (6)) underestimated the decrease in the strain at break by the incorporation of fillers. The Mitsuishi model (orange curve, equation (7)) with the constant A set to 3 predicted the evolution of the strain at break rather well for the individual compounds BN10 (measured: 3.6 % ; calculated: 4 %), G10 (measured: 3.9 %; calculated: 4 %); EG5 (measured: 2.2 %; calculated: 2.1 %). However, it failed to estimate the evolution of the strain at curve of any entire material class as it could not predict the plateau at the higher filler contents above 10 vol%.

3.1.1.3. Ultimate tensile strength

In Figure 5 the ultimate tensile strength of the HDPE-based compounds containing different types of fillers along with the estimation according to equation (8) and (9) are given.

An ultimate tensile strength for the unfilled HDPE of 24.6 MPa was obtained. By the incorporation of fillers, the ultimate tensile strength decreased for all compounds with increasing filler content. Whereas the ultimate tensile strength decreased the least for the compounds containing boron nitride and natural graphite, it decreased to a further extent for the compounds containing aluminum, expanded graphite and copper. The ultimate tensile strength was decreased to 18.8 MPa, 19.9 MPa, 20.1 MPa for the BN10, BN20, BN30 and to 20.1 MPa, 19.5 MPa, 19 MPa for the G10, G20, G30. It was decreased to 17.8 MPa, 12.1 MPa, 13.2 MPa for the A10, A20, A30, to 17.1 MPa, 17.2 MPa, 15.3 MPa, 14.4 MPa, 13.8 MPa for the EG3, EG5, EG10, EG20, EG30, and to 11.1 MPa, 12.1 MPa, 11.6 MPa for the C10, C20, C30, respectively. For all compounds, the major decrease in the ultimate tensile strength was already detected after the incorporation of 10 vol%. Whereas the ultimate tensile strength of G10, BN10 and A10 was reduced by approximately 20 % – 30 %, it was reduced by 38 % for the EG10 and 55 % for the C10. The highest decrease in the ultimate tensile strength was therefore detected for the copper-filled HDPE.

At filler contents between 10 vol% and 30 vol%, the ultimate tensile strength stayed within plateau. Thus, in case the highest possible thermal conductivity is required, a filler content of 30 vol% could be chosen.

As the first power law clearly underestimated the decrease in the ultimate tensile strength, it is not displayed in Figure 5. Equation (8) with B=1.21 predicted the decrease in ultimate tensile strength well for several individual compounds: G10 (measured: 20.1 MPa; calculated: 18.2 MPa), BN10 (measured: 20.1 MPa; calculated: 18.2 MPa), A10 (measured: 17.1 MPa; calculated: 18.2 MPa), EG20 (measured: 14.4 MPa; calculated: 14.4 MPa) and C30 (measured: 11.6 MPa; calculated: 11.2 MPa). However, it did not predict the evolution of the ultimate tensile strength well for an entire material class. It therefore did not prove to be an adequate model to predict the ultimate tensile strength.

By setting the constant C which represents the formation of stress concentrations for the porosity model to 2 and 10, the ultimate tensile strength could be estimated well for the lower filler contents

for the compounds containing natural graphite (smallest decrease in ultimate tensile strength) and of the compounds containing expanded graphite (largest decrease in ultimate tensile strength). However, for the higher filler contents of 20 vol% and 30 vol%, the model overestimates the decrease in the ultimate tensile strength.

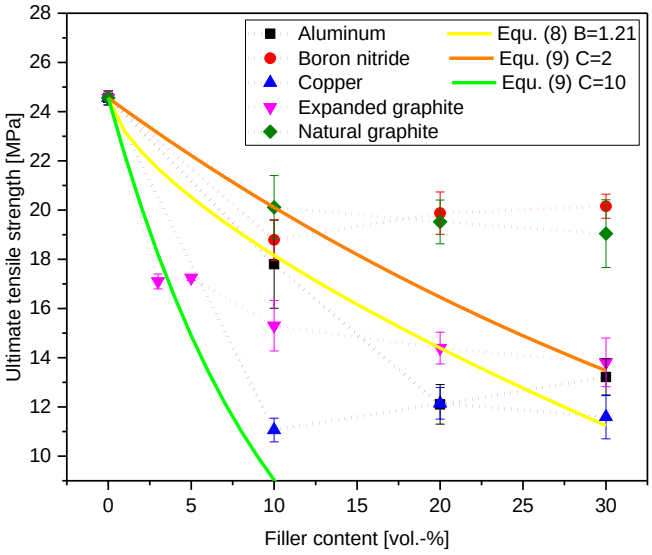

Figure 5: Ultimate tensile strength of HDPE-based compounds containing different types of fillers at filler contents up to 30 vol%. It decrease with increasing filler content for all compounds.

3.1.2. Charpy impact testing

The results from the Charpy impact testing (Charpy impact strength of unnotched specimens, Charpy impact strength of notched specimen, notch sensitivity) of the HDPE-based compounds are given in the following. The individual results are connected by a dotted line to guide the eye but do not represent a function.

3.1.2.1. Charpy impact strength of unnotched specimens

In Figure 6 the Charpy impact strength of the unnotched specimens for the HDPE-based compounds containing different fillers of up to 30 vol% is given. For the HDPE-based compounds containing expanded graphite as filler, the results from the compounds contain 3 vol% and 5 vol% of the large EG particles are additionally given.

An initial impact strength of 23 kJ/m² was obtained. It decreased by the incorporation of fillers to 2.3 kJ/m² and to 1.8 kJ/m² for the A20 and A30, to 8 kJ/m², 4.1 kJ/m², 3 kJ/m² for the BN10, BN20, BN30, to 5.1 kJ/m², 2.3 kJ/m², 2.3 kJ/m² for the C10, C20, C30, to 6.3 kJ/m², 4.7 kJ/m², 2.5 kJ/m², 1.8 kJ/m², 1.7 kJ/m² for the EG3, EG5, EG10, EG20, EG30, and to 8 kJ/m², 3.6 kJ/m², 2.2 kJ/m² for the G10, G20, G30, respectively. The impact strength decreased the most after adding 10 vol%. For both compounds, G10 and BN10, it was decreased by approximately 65 %, whereas a higher decrease of approximately 80 % and 90 % for the C10 and EG were found, respectively. However, the additionally given data points for the EG3 and EG5 exhibit large decrease in impact strength already at a filler content of 3 vol%. This might indicate that the major embrittlement occurs at lower filler contents also for the compounds containing other types of fillers (aluminum, boron nitride, copper and natural graphite). At the higher filler contents of 20 vol% and 30 vol%, similar results independent of the type of filler were found and the impact strength reached a plateau for the different types of compounds.

The decrease in impact strength represents an increase in the embrittlement as less energy can be absorbed by the material. Typically, a polymer with a high impact strength absorbs most of the impact energy and exhibits a low crack propagation rate. In two-phase systems, however, the crack propagation rate is increased along the particle-polymer interface due to a weak adhesion between the filler and the polymer[7].

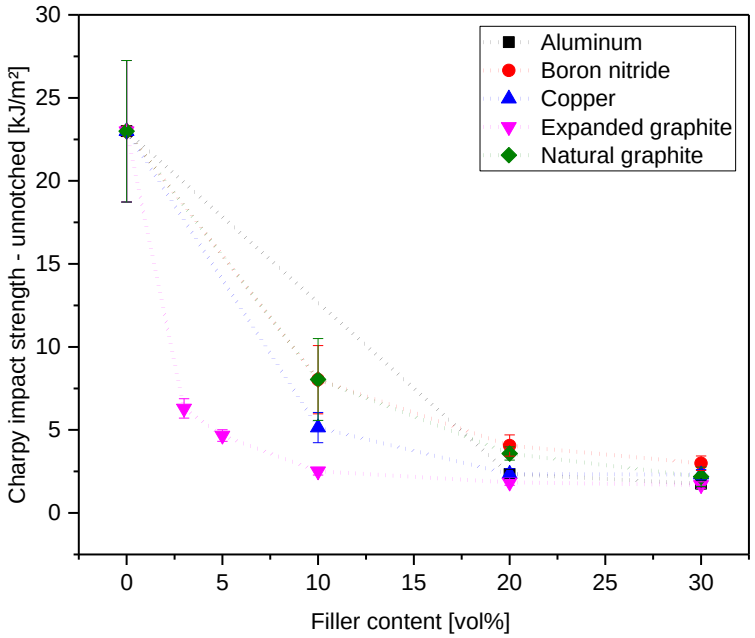

Figure 6: Charpy impact strength of unnotched specimen for HDPE-based compounds containing different fillers up to 30 vol%. The impact strength decreased with increasing filler content for all compounds.

3.1.2.2. Charpy impact strength of notched specimens

In Figure 7 the Charpy impact strength of the notched specimens for the HDPE-based compounds containing different fillers of up to 30 vol% is given. For the HDPE-based compounds containing expanded graphite as filler, the results from the compounds contain 3 vol% and 5 vol% of the large EG particles are additionally displayed.

The initial impact strength of the unfilled HDPE was found to be 3.2 kJ/m². According to the material data sheet the impact strength of the HDPE is 4 kJ/m². Considering the differences in the specimen preparation (compression molding vs. injection molding), the generated impact strength was in reasonable agreement with the one from the material data sheet.

As seen with the unnotched specimens, the impact strength of the compounds was decreased by the incorporation of the different types of fillers with the notched specimens. It was decreased to 2.1 kJ/m², 2 kJ/m², 1.7 kJ/m² for the A10, A20, A30, to 1.5 kJ/m², 1.2 kJ/m², 1.2 kJ/m² for the BN10, BN20, BN30, to 2.6 kJ/m², 2 kJ/m², 2.2 kJ/m² for the C10, C20, C30, to 2.4 kJ/m², 2.1 kJ/m², 1.8 kJ/m², 1.6 kJ/m², 1.5 kJ/m², for the EG3, EG5, EG10, EG20, EG30, and to 1.5 kJ/m², 1.5 kJ/m², 1.4 kJ/m² for the G10, G20, G30, respectively.

A major decrease in impact strength of the notched specimen was detected at a filler content of 10 vol%: approximately 20 % for the C10, 35 % for the A10, 45 % for the EG10 and 55 % for the BN10 and G10. However, only the compound containing natural graphite reached a plateau at the higher filler contents of 20 vol% and 30 vol% as it was seen for the unnotched specimens in Figure 6.

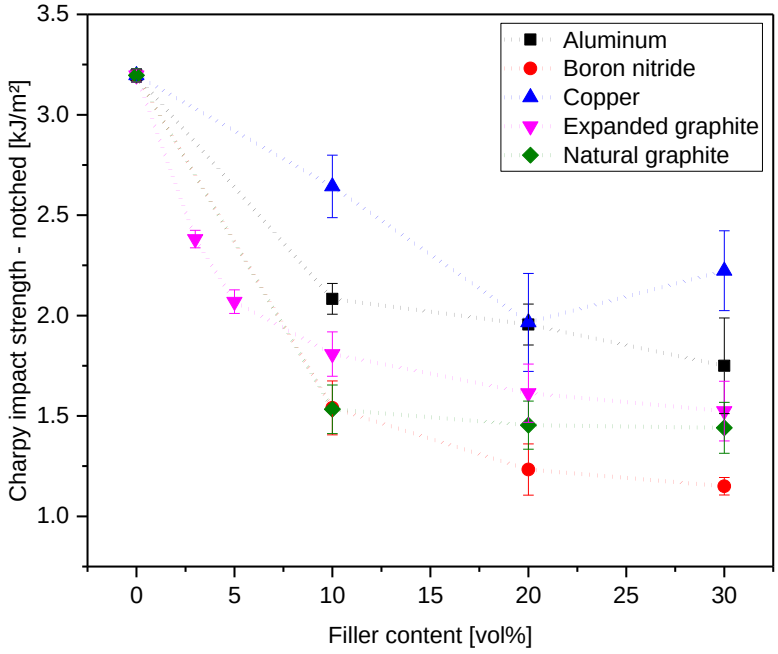

Figure 7: Charpy impact strength of notched specimens for HDPE-based compounds containing different fillers up to 30 vol%. The impact strength decreased for all compounds.

3.1.2.3. Notch sensitivity

In Figure 8 the notch sensitivity of the HDPE-based compounds containing different fillers of up to 30 vol% is displayed. With increasing filler content, the notch sensitivity increased for all compounds. For the HDPE-based compounds containing aluminum and copper, a notch sensitivity of almost 100 % was reached at a filler content of 30 vol%. This resulted from the similar impact strength of the unnotched and the notched specimen.

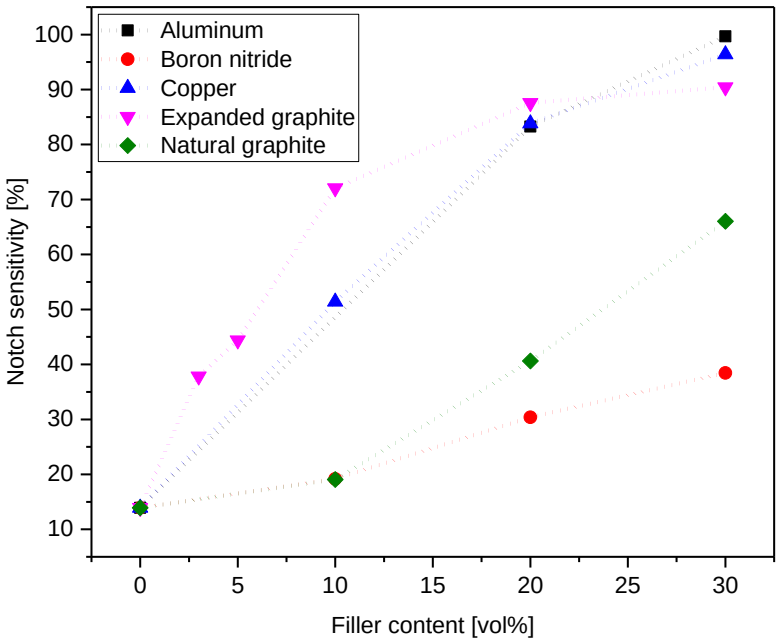

Figure 8: Notch sensitivity of HDPE-based compounds containing different fillers of up to 30 vol%. It increased with increasing filler content.

3.2. Processing impact

3.2.1. Tensile testing

The results from the tensile testing of the HDPE-based compounds containing three different types of expanded graphite (EG-S, EG-M, EG-L) which were processed in two different ways are given in the following. The mechanical characteristics (Young's modulus, strain at break, ultimate tensile strength) are given separately depending on their type of processing (one figure for direct processing, one figure for processing via masterbatch). The individual data points are connected via a dotted line to guide to eye.

3.2.1.1. Young's modulus

The Young's modulus of the HDPE-based compounds containing three different types of expanded graphite (EG-S, EG-M, EG-L) which were processed directly and via masterbatch are given in Figure 9a and b, respectively. By the incorporation of the expanded graphite particles, the Young's modulus increased for all compounds with increasing filler content. It increased from 1640 MPa for the unfilled HDPE to 2290 MPa and 2220 MPa for the EG-S-5-dir and the EG-S-5-MB, to 2150 MPa and 2220 MPa for EG-M-5-dir and the EG-M-5-MB, to 2360 MPa and 2150 MPa, for the EG-L-5-dir and the EG-L-5-MB, respectively. However, no tendency regarding the particle size could be detected as the data scattering was too large and the standard deviations partially overlapped.

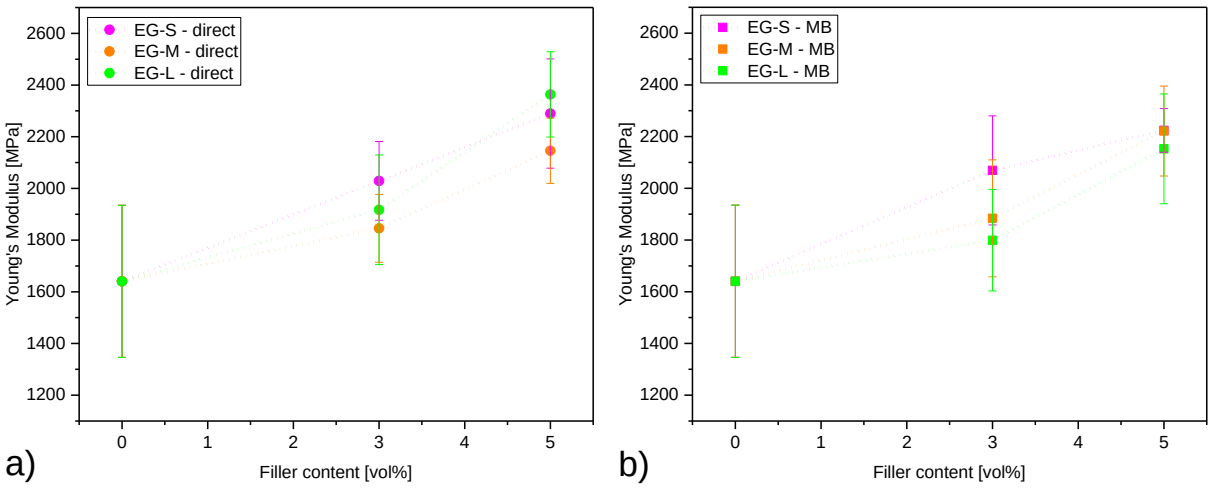

Figure 9: The Young's modulus of HDPE-based compounds containing three different types of expanded graphite: a) processed directly; b) processed via masterbatch.

3.2.1.2. Strain at break

The strain at break of the HDPE-based compounds containing three different types of expanded graphite (EG-S, EG-M, EG-L) which were processed directly and via masterbatch are given in Figure 10a and b, respectively. For all compounds, the strain at break decreased with increasing filler content. When processed directly, it decreased from 11.2 % for the unfilled HDPE to 3.2 %, 2.1 % and 2.2 % for the EG-S, EG-M and EG-L at a filler content of 5 vol%. When processed via masterbatch, it decreased from 11.2 % for the unfilled HDPE to 3.4 %, 2.6 % and 2.7 % for the EG-S, EG-M and EG-L at a filler content of 5 vol%.

The strain at break depended on the particle size for the compounds for the compounds which were processed directly (Figure 10a). The small EG-S graphite particles yielded the highest strain at break.

Considering that the particles are defects within the continuous HDPE matrix which act as crack initiator, smaller defects evoke smaller stress concentrations sites compared to the larger particles. Thereby the break occurred at higher elongations for the compounds with the small particles.

When comparing both processing types, the processing via masterbatch yielded higher values for the strain at break. The expanded graphite particles were sheared twice during the manufacturing of these compounds. Thus the particles within the HDPE matrix were smaller when processed via masterbatch (Figure 11b) than the particles when processed directly (Figure 11a) as the expanded graphite was sensitive towards the applied shear. Thus, smaller particles yielded a higher strain at break. This was in good agreement with the detected higher strain at break for the directly processed compounds that contained the small particles. Furthermore, the additional shearing seemed to diminished the differences in the mechanical properties as the particles were all crushed. Thus, smaller gaps between the individual results of the strain at break for the compounds which were processed via masterbatch were detected.

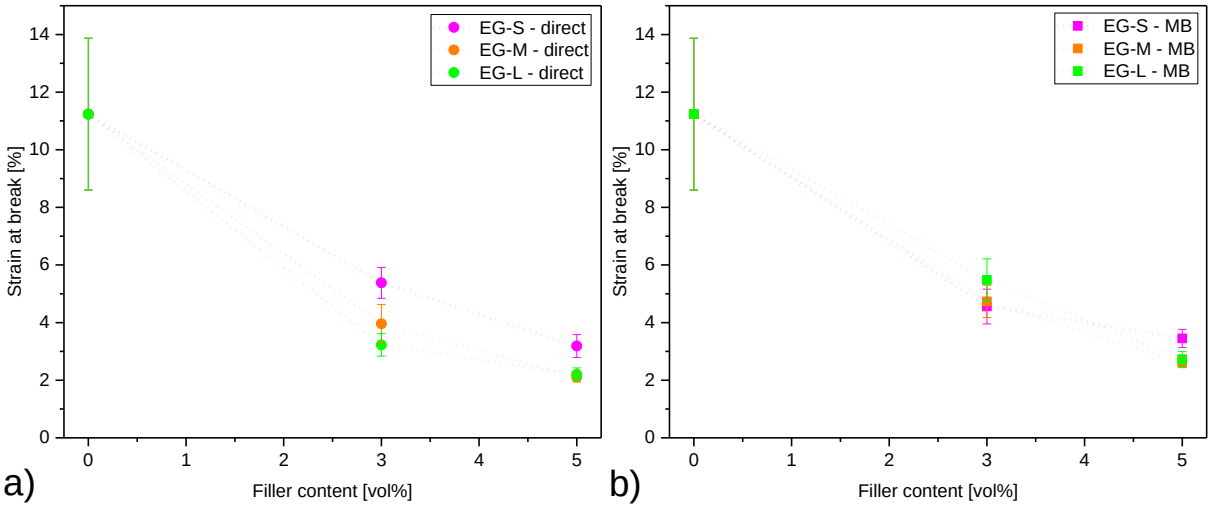

Figure 10: The strain at break of HDBE-based compounds containing three different types of expanded graphite: a) processed directly; b) processed via masterbatch. The strain at break decreased for all HDPE-based compounds with increasing filler content. Smaller particles yielded a higher strain at break.

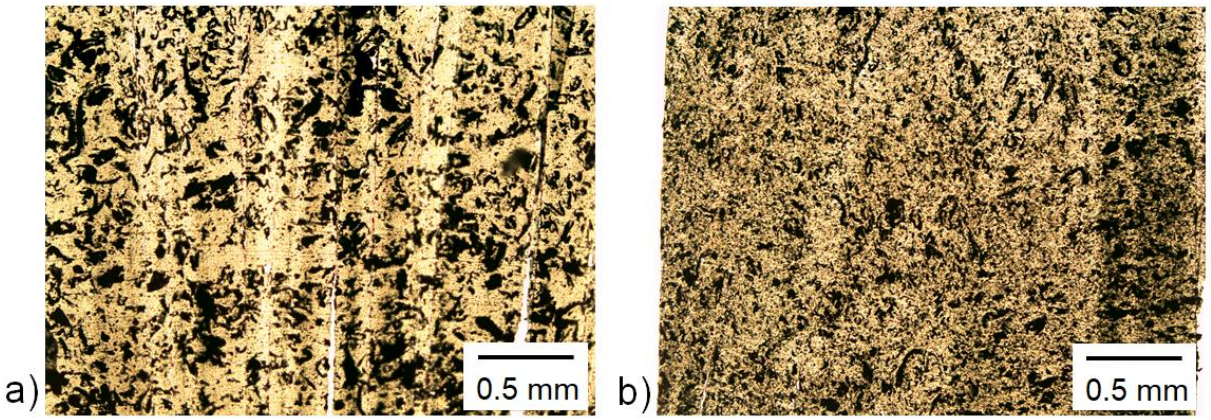

Figure 11: Micrographs of the HDPE-based compounds containing 3 vol% of the large expanded graphite particles EG-L recorded via transmitted light-microscopy: a) the compound was processed directly and the expanded particles were larger

since they were only sheared once; b) the compound was processed via masterbatch. The expanded graphite particles were sheared twice and were

Interestingly, only small differences in the strain at break between the compounds containing the medium-sized (EG-M) and large (EG-L) particles were found. This was also the case for the enhancement in thermal conductivity (not displayed here). The micrograph of the compound containing 3vol% of the medium-sized particles EG-M is displayed in Figure 12a. The size distribution between the EG-M-3-dir and the EG-L-3-dir (Figure 11a) are comparable. Thus, the first round of shearing downsized the EG-M and EG-L to approximately the same size of particles which caused similar mechanical behavior.

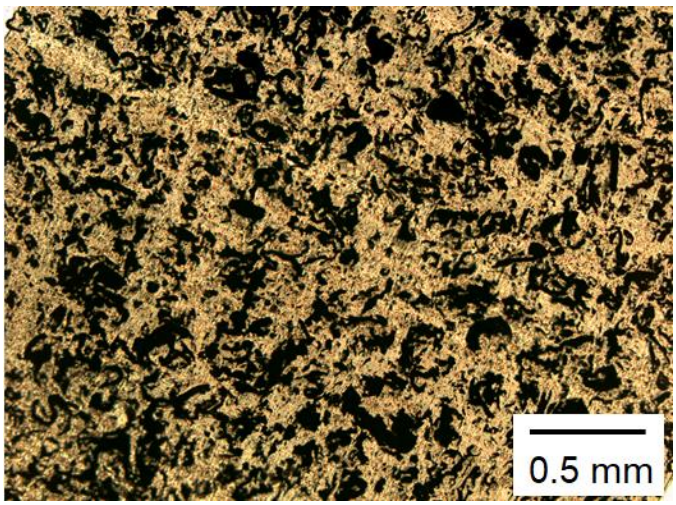

Figure 12: Micrograph of the HDPE-based compound containing 3 vol% of the medium-sized expanded graphite particles EG-M recorded via transmitted light-microscopy. The compound was only sheared once. The particles possess a similar size distribution as the HDPE-based compound containing 3 vol% of the large expanded graphite particles EG-L given in Figure 11a.

3.2.1.3. Ultimate tensile strength

The ultimate tensile strength of the HDPE-based compounds containing three different types of expanded graphite (EG-S, EG-M, EG-L) which were processed directly and via masterbatch are given in Figure 13a and b, respectively. For all compounds, the ultimate tensile stress decreased from 24.6 MPa for the unfilled HDPE to 19.5 MPa, 16.7 MPa, 17.2 MPa for the EG-S, EG-M and EG-L at a filler content of 5 vol% when processed directly. When processed via masterbatch, it decreased to 20.3 MPa, 19.5 MPa, 19.9 MPa for the EG-S, EG-M and EG-L at a filler content of 5 vol%.

For both processing types, the particle size affected the ultimate tensile strength. The small EG-S particles provoked a higher ultimate tensile strength when compared to the medium-sized EG-M and the large EG-L particles. This was again attributed to the comparably smaller defects caused by the smaller particles within the matrix as smaller stress concentrations were present. However, this effect was more pronounced for the compounds processed directly. As shown in Figure 11 and Figure 12 and discussed in 3.2.1.2, the differences in particle sizes were larger for the compounds that were processed directly as the particles had undergone only one round of shearing. This explains the more pronounced impact of the particle size on the compounds which were processed directly.

The processing via masterbatch yielded a higher ultimate tensile strength for all compounds than the direct processing. As discussed above, the additional extrusion round reduced the particle size and smaller stress concentrations within the polymeric matrix were present. Thus, a higher ultimate tensile strength was detected.

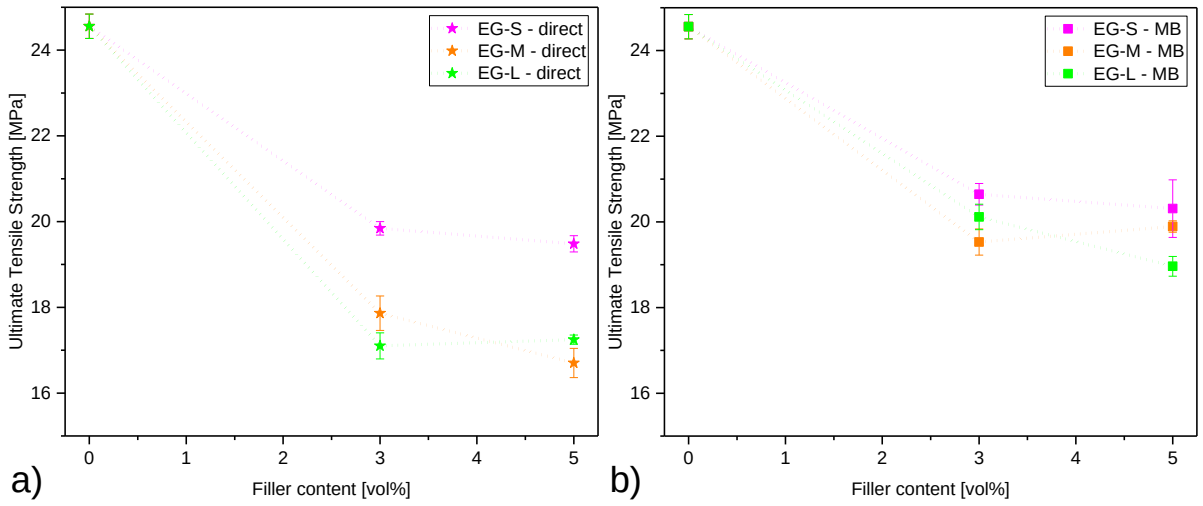

Figure 13: The ultimate tensile strength of HDPE-based compounds containing three different types of expanded graphite: a) processed directly; b) processed via masterbatch.

3.2.2. Charpy impact testing

3.2.2.1. Charpy impact strength of unnotched specimens

The Charpy impact strength of the unnotched specimens for the HDPE-based compounds containing three different types of expanded graphite (EG-S, EG-M, EG-L) which were processed directly and via masterbatch are given in Figure 14a and b, respectively. A Charpy impact strength of 23 kJ/m² was obtained for the unfilled HDPE. For all compounds, the impact strength decreased by the incorporation of the graphite particles. For the compounds which were processed directly, it decreased to 5.3 kJ/m², 4.1 kJ/m², 4.7 kJ/m², for the EG-S, EG-M, EG-L, respectively, at the maximum filler content of 5 vol%. For the compounds which were processed via masterbatch, it decreased to 1.8 kJ/m², 2.4 kJ/m², 4.4 kJ/m² for the EG-S, EG-M, EG-L, respectively, at the maximum filler content of 5 vol%.

Only very small differences for the compounds which were processed directly could be found (Figure 14a). The incorporation of the smallest graphite particles EG-S evoked a slightly higher impact strength at 3 vol% (8.6 kJ/m²) and at 5 vol% (5.3 kJ/m²) over the incorporation of the medium-sized and large particles EG-M and EG-L at 3 vol% (6.7 kJ/m² and 6.37 kJ/m²) and at 5 vol% (4.1 kJ/m² and 4.7 kJ/m²). However, this trend was not observed for the compounds processed via masterbatch where the results and their deviation overlapped for all compounds. Presumably, no difference in the impact strength of the unnotched specimen could be detected because of the uncontrolled crack propagation.

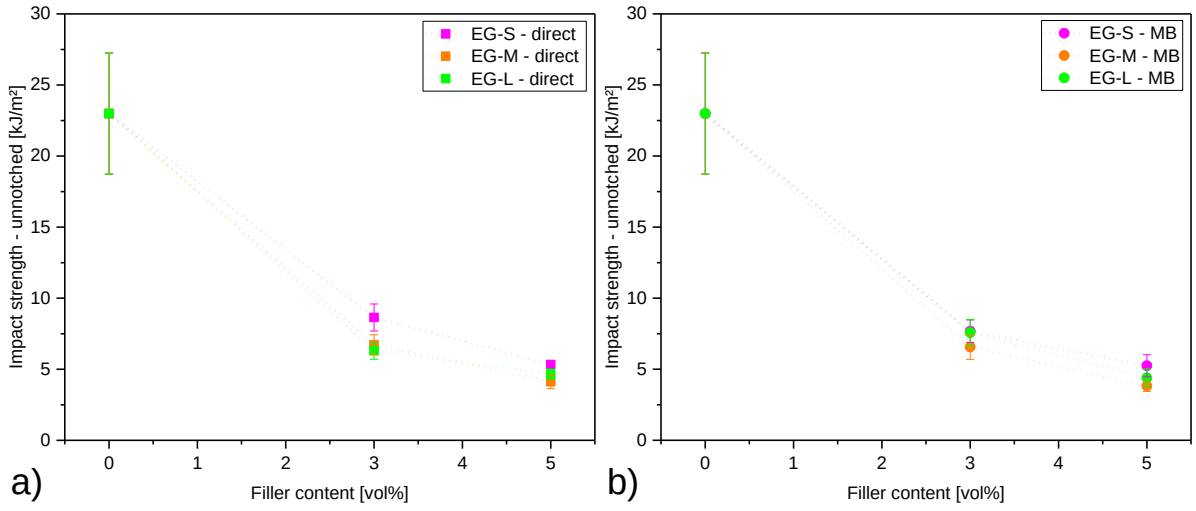

Figure 14: Charpy impact strength of the unnotched specimens for the HDPE-based compounds containing three different types of expanded graphite: a) processed directly; b) processed via masterbatch.

3.2.2.2. Charpy impact strength of notched specimens

The Charpy impact strength of the notched specimens for the HDPE-based compounds containing three different types of expanded graphite (EG-S, EG-M, EG-L) which were processed directly and via masterbatch are given in Figure 15a and b, respectively. A Charpy impact strength of 3.2 kJ/m² was obtained for the unfilled HDPE. For all compounds, it decreased by the incorporation of the graphite particles. For the compounds which were processed directly, it decreased to 1.8 kJ/m², 2 kJ/m², 2.1 kJ/m², for the EG-S, EG-M, EG-L, respectively, at the maximum filler content of 5 vol%. For the compounds which were processed via masterbatch, the impact strength decreased to 1.4 kJ/m², 1.2 kJ/m², 1.6 kJ/m², for the EG-S, EG-M, EG-L, respectively, at the maximum filler content of 5 vol%.

For the compounds which were processed directly the particle size affected the impact strength. The incorporation of the small EG-S particles yielded a lower impact strength than the incorporation of the medium-sized EG-M and the large EG-L particles. Considering that more individual small particles have to be dispersed within the polyethylene matrix in order to reach the same filler content than the medium-sized and large particles, there is less continuous polymeric volume available. A small polymeric volume can absorb only little of the energy applied during the impact more easily as there is less volume that can be deformed. Thus, a further decrease in the impact strength was detected for all the compounds which were processed via masterbatch as all particles were sheared into smaller particles and thereby interrupted the continuous polymer volumes more often.

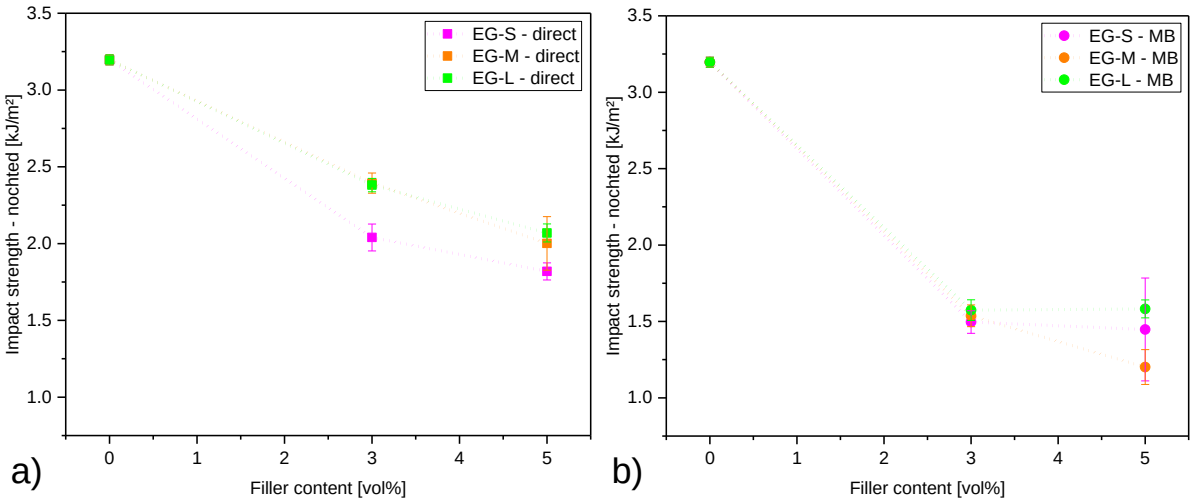

Figure 15: Charpy impact strength of the unnotched specimens for the HDPE-based compounds containing three different types of expanded graphite: a) processed directly; b) processed via masterbatch.

4. Summary and outlook

In the first part of the study, the mechanical properties of high-density polyethylene (HDPE) based compounds containing five different types of fillers (aluminum, boron nitride, copper, expanded graphite, natural grahite) of up to 30 vol% were examined. Tensile testing gave the compounds' Young's modulus, the strain at break and the ultimate tensile strength. Additionally, several models for predicting the material behavior were applied and adapted to the evolution of the mechanical properties of the different compounds. Via Charpy impact testing, the impact strength of unnotched and notched specimens and the notch sensitivity were determined.

The Young's modulus of all compounds increased with increasing filler content as their stiffness increased. For both, the ultimate tensile strength and the strain at break, a decrease was detected for all compounds. The major decrease in the ultimate tensile strength and the strain at break occurred after the incorporation of 10 vol% of filler. At the higher filler contents of 20 vol% and 30 vol%, the ultimate tensile strength and the strain at break reached a plateau and both characteristics did not decrease further. The applied models to predict the Young's modulus (Einstein's equation, Guth equation, Thomas equation), the ultimate tensile strength (Bigg's model, porosity model) and the strain at break (Nielsen model, Mitsuishi equation) were either in good agreement with individual results or could be adapted via constants to match the mechanical properties of the compounds at low filler contents. However, they failed to predict the mechanical properties of an entire material class. The Charpy impact strength for both, the unnotched and the notched specimens, was decreased by the incorporation of fillers. Whereas the major decrease in the impact strength was detected after adding 10 vol% for the unnotched specimens, the impact strength decreased further at higher filler contents for the notched specimens.

The second part of the present study focused on the processing impact of compounds containing expanded graphite as filler which is sensitive towards shear. Three different types of expanded graphite with different particle sizes (small, medium-sized and large) were processed directly and via masterbatch at filler contents of 3vol% and 5vol%.

No impact of the initial particle size or the processing was detected for the Young's modulus. However, a higher strain at break and ultimate tensile strength were ascertained for the directly processed compounds which contained the small expanded graphite particles. This was partially also detected for the compounds which were processed via masterbatch but only to a smaller extent. When looking at the processing impact, masterbatch processing yielded a higher strain at break and a lower ultimate tensile strength than direct processing. This was attributed to the reduction in the particle size via the additional extrusion round of the masterbatch processing. Thus, it was observed twice that small expanded graphite particles evoked a smaller strain at break and ultimate tensile strength. This was attributed to the resulting smaller stress concentration sites. For the Charpy impact testing of the unnotched specimens, no tendencies regarding the initial particle size or the type of processing were detected. This was probably due to uncontrolled crack propagation as the comparably large expanded graphite particles acted as obstacles. The notching of the specimens, however, helped to define the crack propagation and the Charpy impact testing of the notched specimens revealed a dependency on the initial particle size of the directly processed particles and on the processing type. Compounds which contained small particles (either because of the initial difference in the particle size or the reduction in particle size via masterbatch processing) exhibited a lower impact strength. This was attributed to smaller continuous polymeric volumes which could absorb less impact energy via deformation.

The detected impacts on the mechanical properties for the compounds containing expanded graphite could be explained with the differences in particles sizes between the fillers. However, the mechanical properties of semi-crystalline polymers are typically also strongly depending on their crystalline morphology. Filler particles tend to affect the crystalline structure of the surrounding semi-crystalline polymeric matrix (e.g. as nucleating agents). Thus, measurement techniques for investigating the crystalline structure of the compounds (e.g. differential scanning calorimetry and small angle scattering) could help to further analyze the origin of the detected impacts.

5. References

[1] T. A. Osswald, E. Baur, S. Brinkmann, K. Oberbach, E. Schmachtenberg, *International Plastics Handbook.* Carl Hanser Verlag GmbH & Co. KG, München **2006**.

[2] I. H. Tavman, *International communications in heat and mass transfer.* **1998**, *25*, 723.

[3] I. Krupa, I. Chodák, *European polymer journal.* **2001**, *37*, 2159, DOI: 10.1016/S0014-3057(01)00115-X.

[4] I. H. Tavman, *Powder Technology.* **1997**, *91*, 63, DOI: 10.1016/S0032-5910(96)03247-0.

[5] I. H. Tavman, *J. Appl. Polym. Sci.* **1996**, *62*, 2161, DOI: 10.1002/(SICI)1097-4628(19961219)62:12<2161::AID-APP19>3.0.CO;2-8.

[6] A. Einstein, *Ann. Phys.* **1905**, *14*, 182, DOI: 10.1002/andp.200590005.

[7] Rusu, M., Sofian, N., & Rusu, D, *Polymer Testing.* **2001**, *20*, 409.

[8] L. E. Nielsen, *J. Appl. Polym. Sci.* **1966**, *10*, 97, DOI: 10.1002/app.1966.070100107.

[9] K. Ghosh, S. N. Maiti, *J. Appl. Polym. Sci.* **1996**, *60*, 323, DOI: 10.1002/(SICI)1097-4628(19960418)60:3<323::AID-APP5>3.0.CO;2-N.

[10] K. Mitsuishi, S. Kodama, H. Kawasaki, *Polym. Eng. Sci.* **1985**, *25*, 1069, DOI: 10.1002/pen.760251704.

[11] L. E. Nielsen, R. F. Landel, *Mechanical properties of polymers and composites.* CRC Press, Boca Raton, Florida **1993**.

[12] D. M. Bigg, *Polym. Eng. Sci.* **1979**, *19*, 1188, DOI: 10.1002/pen.760191610.

[13] G. W. Ehrenstein, G. Riedel, P. Trawiel, *Thermal analysis of plastics: Theory and practice.* Hanser, Munich **2004**.